Journal of the American College of Cardiology
© 2005 by the American College of Cardiology Foundation
Published by Elsevier Inc.

Vol. 45, No. 12, 2005
ISSN 0735-1097/05/$30.00
doi:10.1016/j.jacc.2005.02.082

Cardiac Imaging

Measurement of Ventricular Torsion by Two-Dimensional Ultrasound Speckle Tracking Imaging

Yuichi Notomi, MD* Peter Lysyansky, PHD,‡ Randolph M. Setser, DSC,† Takahiro Shiota, MD, FACC,* Zoran B. Popović, MD,* Maureen G. Martin-Miklovic, Joan A. Weaver, RT,* Stephanie J. Oryszak,* Neil L. Greenberg, PHD, FACC,* Richard D. White, MD,*† James D. Thomas, MD, FACC*

Cleveland, Ohio; and Tirat Hacarmel, Israel

OBJECTIVES We sought to examine the accuracy/consistency of a novel ultrasound speckle tracking imaging (STI) method for left ventricular torsion (LVtor) measurement in comparison with tagged magnetic resonance imaging (MRI) (a time-domain method similar to STI) and Doppler tissue imaging (DTI) (a velocity-based approach).

BACKGROUND Left ventricular torsion from helically oriented myofibers is a key parameter of cardiac performance but is difficult to measure. Ultrasound STI is potentially suitable for measurement of angular motion because of its angle-independence.

METHODS We acquired basal and apical short-axis left ventricular (LV) images in 15 patients to estimate LVtor by STI and compare it with tagged MRI and DTI. Left ventricular torsion was defined as the net difference of LV rotation at the basal and apical planes. For the STI analysis, we used high-frame (104 ± 12 frames/s) second harmonic two-dimensional images.

RESULTS Data on 13 of 15 patients were usable for STI analysis, and LVtor profile estimated by STI strongly correlated with those by tagged MRI ($y = 0.95x + 0.19$, $r = 0.93$, $p < 0.0001$, analyzed by repeated-measures regression models). The STI torsional velocity profile also correlated well with that by the DTI method ($y = 0.79x + 2.4$, $r = 0.76$, $p < 0.0001$, by repeated-measures regression models) with acceptable bias.

CONCLUSIONS The STI estimation of LVtor is concordant with those analyzed by tagged MRI (data derived from tissue displacement) and also showed good agreement with those by DTI (data derived from tissue velocity). Ultrasound STI is a promising new method to assess LV torsional deformation and may make the assessment more available in clinical and research cardiology. (J Am Coll Cardiol 2005;45:2034–41) © 2005 by the American College of Cardiology Foundation

Current research in clinical cardiac mechanics is moving from short- and long-axis left ventricular (LV) function and ejection fraction to three-dimensional ventricular deformation studies, including left ventricular torsion (LVtor) (1). In systole, the LV apex rotates counterclockwise (as viewed from the apex), whereas the base rotates clockwise, creating a torsional deformation originating in the dynamic interaction of oppositely wound epicardial and endocardial myocardial fiber helices. Although this wringing motion (systolic twisting and early diastolic untwisting) can give novel insights into LV function that cannot be obtained from standard short- and long-axis analysis, it has proven difficult to measure. Previous investigators approached LV rotation (LVrot)/LVtor using short-axis echo scans to track macroscopically the movement of distinguishable anatomic landmarks such as papillary muscle or mitral valve (2,3).

One of the special characteristics of static B-scan ultrasound imaging is an appearance of speckle patterns within the tissue, which are the result of constructive and destructive interference of ultrasound back-scattered from structures smaller than a wavelength of ultrasound (4). Motion analysis by speckle tracking has been attempted using block-matching and autocorrelation search algorithms (5–7), and speckle motion has been closely linked to underlying tissue motion when small displacements are involved (6). On the basis of this displacement estimation technique, LVrot (angle-displacement about the central axis of LV in the short-axis view) for assessment of LVtor can be measured.

A newly developed speckle tracking imaging (STI) technique has presented us the possibility of enhancing the accuracy of displacement estimation by filtering out random speckles and then performing autocorrelation to estimate motion of stable structures (8–10). This non-Doppler assessment of cardiac mechanics could rival magnetic resonance imaging (MRI) or Doppler tissue imaging (DTI) in measuring LVtor and may prove more versatile in assessing patients in clinical and research settings. Therefore, we sought to examine the accuracy/consistency of the STI method for LVtor measurement in comparison with tagged MRI (a time-domain method

From the Departments of *Cardiovascular Medicine and †Radiology, The Cleveland Clinic Foundation, Cleveland, Ohio; and ‡GE Ultrasound Israel Ltd, Tirat Hacarmel, Israel. Dr. Notomi is funded through a postdoctoral fellowship grant of the Ohio Valley affiliate of the American Heart Association (0325237B) and the current study is a part of the grant. This study also was supported in part by the National Aeronautics and Space Administration (Houston, Texas, Grant NCC9-58) and the Department of Defense (Fort Dietrich, Maryland, USAMRMC Grant #02360007).

Manuscript received December 13, 2004; revised manuscript received February 7, 2005, accepted February 22, 2005.

Abbreviations and Acronyms

CV	= coefficient of variation
DTI	= Doppler tissue imaging
LV	= left ventricular
LVrot	= left ventricular rotation
LVrot-v	= left ventricular rotational velocity
LVtor	= left ventricular torsion
LVtor-v	= left ventricular torsional velocity
MRI	= magnetic resonance imaging
STI	= speckle tracking imaging

similar to STI) and DTI (a velocity-based approach), a method recently validated by our group (11).

METHODS

Study population. We assessed LVtor in consecutive patients undergoing clinically indicated cardiac MRI studies. The research echocardiographic study was performed on the same day as the MRI, and "technically difficult cases" for transthoracic echocardiographic examination were pre-excluded (one or two patients). Fifteen patients with a variety of cardiac pathologies were recruited in an attempt to cover a broad clinical range of LVtor: coronary artery disease (n = 4), aortic root disorder (n = 8, including 3 patients with severe aortic stenosis, 4 patients with severe aortic insufficiency, and 3 patients after aortic valve replacement), and cardiomyopathies (n = 3). The study protocol was approved by the Institutional Review Board of the Cleveland Clinic Foundation. Written informed consent was obtained before the study from all patients.

Terminology and calculation of LVtor and torsional velocity (LVtor-v). We defined "LV torsion" and "LV torsional velocity" as a net-difference of "LV rotation" and "LV rotational velocity" between apical and basal short-axis planes (normally, the apex rotates counterclockwise whereas the base rotates clockwise when viewed from apex; Fig. 1) obtained from STI, DTI, and MRI. We defined LVrot and LVrot-v as angular displacement and velocity, respectively, of the LV about its central axis in the short-axis image. They were stated in units of degree (°) and degrees per second (°/s), respectively. Counterclockwise LVrot as viewed from apex was expressed as a positive value.

Comparison of STI with DTI/MRI data. For comparison of LVtor derived from STI and MRI, we carefully chose the most similar short-axis images (using size and anatomical landmarks as described below). For comparison of LVtor-v derived from the STI and DTI, we used the images of STI and DTI scanned consecutively by fixed probe. For temporal analysis, the time sequence was normalized to the percent of systole duration (i.e., at end-systole, t was 100%) in all modalities. End-systole was determined from the end of the LV outflow Doppler flow profile in the echocardiography examinations and from the smallest cavity observed in the MRI studies.

Echocardiography. After a clinical standard echocardiographic examination, we scanned apical and basal short-axis planes using a high frame rate (86 to 115 frames/s) second harmonic (transmit/receive: 1.7/3.4 MHz) B-mode (for STI), and DTI mode with a Vivid 7 ultrasound machine (GE Medical Systems, Milwaukee, Wisconsin) with an M3S probe. We defined the proper short-axis levels as

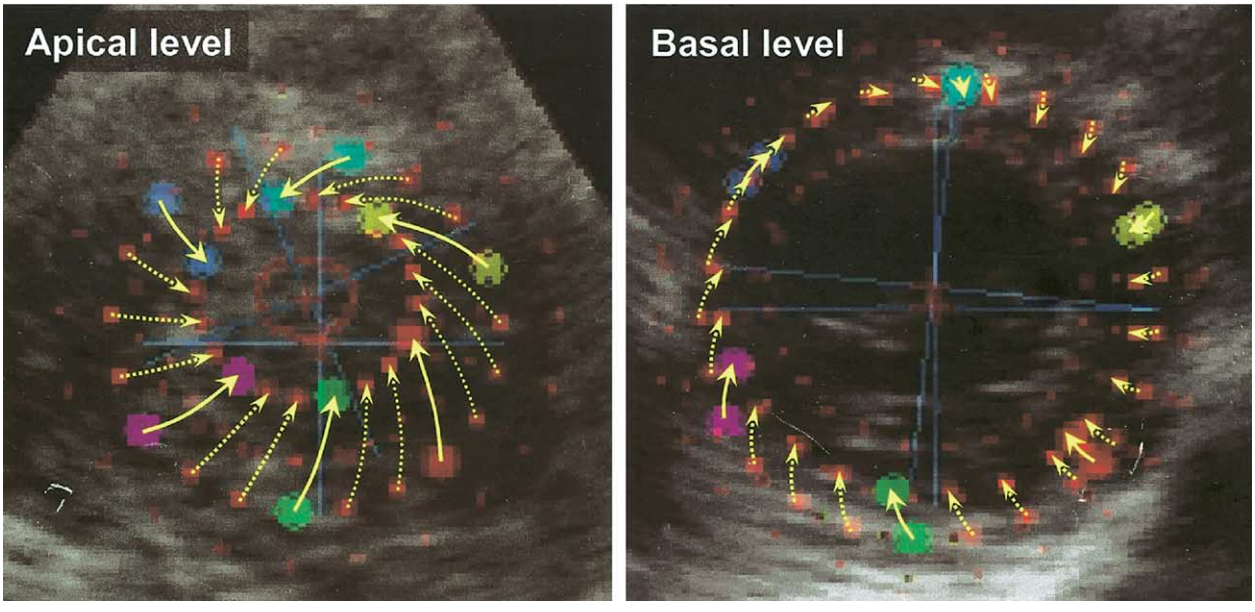

Figure 1. Left ventricular rotation (LVrot) at apical and basal levels during systole by "overlaid" speckle tracking images. End-systolic speckle tracking imaging acquisitions are overlaid on the end-diastolic image with corresponding local trajectories (**tail and head of arrows** indicate the location of end-diastole and end-systole). The LVrot was estimated from all of these regional angle displacements. Normally, at apical level, the left ventricle rotates counterclockwise as viewed from apex, whereas the base rotates clockwise, as in this representative case. This gradient of LVrot between the two levels creates a "wringing" motion of the left ventricle. Videos of speckle tracking imaging in apical and basal short-axis views are available at www.onlinejacc.org.

follows (11): at the basal level, the mitral valve and, at the apical level, LV cavity alone with no visible papillary muscles. The LV cross section was made as circular as possible. The velocity range for DTI was set at 16 or 20 cm/s to prevent aliasing. We used customized software within a personal computer workstation (EchoPAC platform [2DS-software package, version 3.3], GE Medical Systems) for subsequent off-line analysis of STI and DTI.

LV ROTATION AND ROTATIONAL VELOCITY BY STI. Measuring LVrot and LVrot-v by using STI on the workstation is accomplished in five steps: 1) The best-quality digital two-dimensional image cardiac cycle is selected. 2) The endocardium is traced in an optimal frame, from which a speckle tracking region of interest is automatically selected to approximate the myocardium between the endocardium and epicardium (Fig. 2). 3) The region of interest width is adjusted as needed to fit the wall thickness. 4) The computer automatically selects suitable stable objects for tracking and then searches for them in the next frame using the sum of absolute differences algorithm (5,9,10). 5) The speckle tracking algorithm provides a "track score," a reliability parameter based on the degree of decorrelation of the block-matching, shown in each segment as a value from 1.0 to 3.0, with 1 indicating excellent tracking, 2, acceptable, and 3, poor tracking. We excluded segments ≥2.5. After these steps, the workstation computes LVrot and LVrot-v (Figs. 3B and 3C) profiles of each short-axis image (Figs. 1 and 2), defining the ventricular centroid from the midmyocardial line on each frame (Fig. 3A), an approach that is analogous to the MRI analysis described further in this work. The LVrot profile was smoothed temporally with cubic spline interpolation, from which LVrot-v was estimated by differentiation. Averaged ("global") LVrot and LVrot-v data on the midmyocardial contour were used for the calculation for LV torsion. Data plots of the electrocardiogram and the basal and apical LVrot and LVrot-v STI data were exported to a spreadsheet program (Excel 2000, Microsoft Corp, Seattle, Washington) to calculate LVtor.

LV ROTATIONAL VELOCITY BY DTI. Measurement of LVrot-v by tissue Doppler velocity data sets has been validated recently (11). Briefly, LVrot-v is estimated from four points of tissue velocity data on the LV: septal and lateral regions to measure tangential velocity and anterior and posterior region of radial velocity. LVrot-v(t) is estimated from averaged tangential velocity corrected with $r\,(t)$, as follows:

$$LVrot - v(t) = \frac{(Vlat(t) - Vsep(t))/2}{r\,(t)}$$

where $r\,(t)$ is

$$r\,(t) = r_0 + \left\{\int_0^t (Vant(t) - Vpos(t))dt\right\} \Big/ 2$$

and *Vlat*, *Vsep*, *Vant*, and *Vpos* are myocardial velocity at lateral, septal, anterior, and posterior regions, respectively, and r_0 is the end-diastolic radius. The Doppler velocity data sets of the four regions detected by DTI at the basal and apical levels were then transferred to a spreadsheet program for averaging and calculation of LVrot-v and LVtor-v. At least three consecutive cardiac cycles were averaged for these calculations.

MRI. We used a 1.5-T scanner (Sonata, Siemens Medical Solutions, Erlangen, Germany) for the MRI. After scout images were acquired to identify the cardiac axes, several levels of short-axis image loops were acquired during

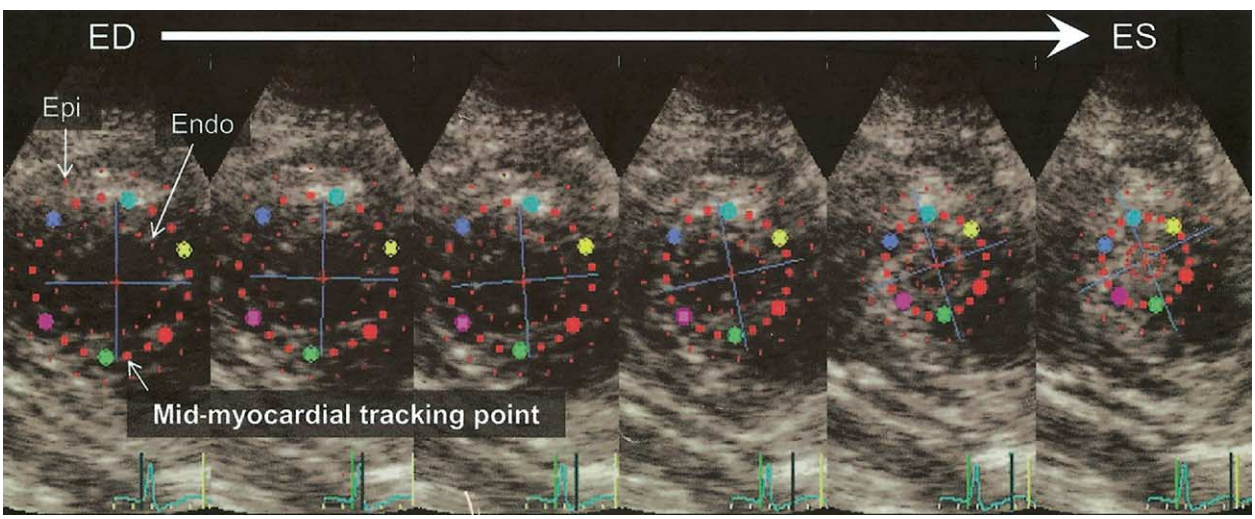

Figure 2. Speckle tracking of successive two-dimensional images obtained from a speckle tracking imaging movie at the apical level during systole in a representative patient. Shown is every sixth frame from successive apical short-axis images, from end-diastole (ED) (onset of QRS of the electrocardiogram) to end-systole (ES), as displayed on the workstation. The **small red dots** depict the endocardial (Endo) and epicardial (Epi) borders, with the midmyocardium shown more boldly, defining the region of interest. The **colored points** track individual locations throughout the cardiac cycle. The left ventricular (LV) centroid is shown as a **small red cross** in the LV cavity and is determined from the midmyocardial line in each frame. The **blue crossed lines** indicate the averaged LV rotation calculated from the angle displacement of all of mid-myocardial dots.

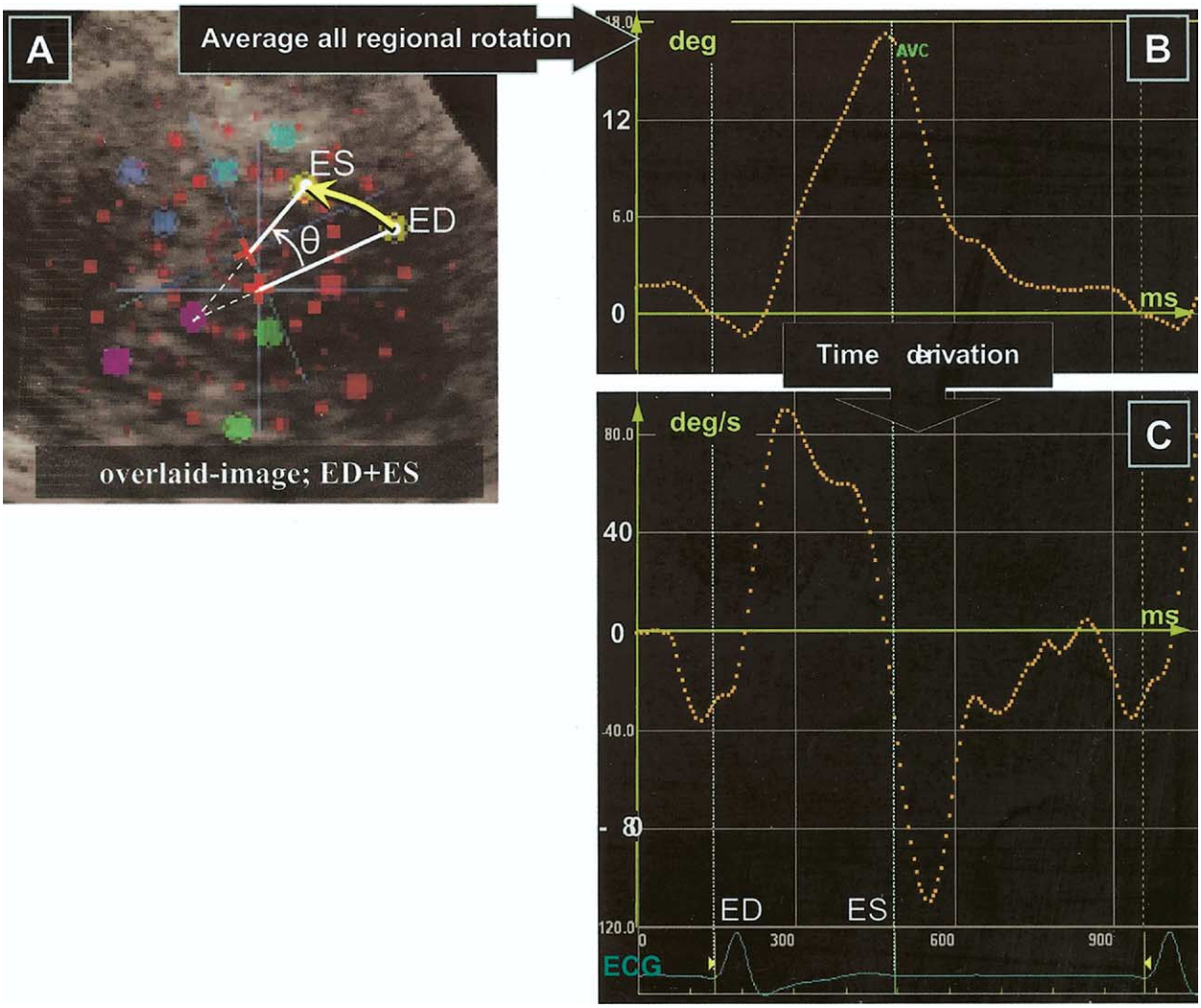

Figure 3. **(A)** Quantification of local angle displacement of the specific region. A representative apical rotation is shown. Regional angle displacement (Θ) was defined by position of a specific tissue element at two different time points and center of the gravity determined by the midmyocardial points. **(B)** and **(C)** Profile curve of left ventricular rotation and rotational velocity in a cardiac cycle displayed on the workstation. Left ventricular rotation was calculated from the average of regional points in the midmyocardium **(B)**. Left ventricular rotational velocity was estimated by time-derivation of the left ventricular rotation profile **(C)**. See Figure 2 legend for definitions of ED, ES, **red cross**, and **blue lines**.

suspended respiration (duration ~15 s) using an electrocardiography-triggered, segmented k-space, grid-tagged gradient echo imaging protocol (spatial modulation of magnetization with tag spacing 8 mm, echo time 2.5 ms, sequence repetition time 75 ms, flip angle 15°, temporal resolution 45 ms, slice thickness 8 to 10 mm, field of view 300 to 360 mm, rectangular field of view 75%, base resolution 256 × 256) (12).

LV ROTATION BY MRI. Processing of tagged MRI images was accomplished using Harmonic Phase (HARP) analysis software (Diagnosoft Inc., Palo Alto, California), the details of which have been described (13) and validated (14) previously. Briefly, HARP uses isolated spectral peaks in the frequency-domain representation of tagged images. The inverse Fourier transform of a spectral peak yields a complex image whose phase is related to cardiac motion in one direction. Analysis of two spectral peaks enables two-dimensional cardiac motion to be determined, including tracking individual points within the myocardium. The LV midwall was specified by manually delineating the endocardium and epicardium at end-systole at each short-axis level; the midwall was then located automatically in all other frames. Points lying on the midwall contour were automatically tracked by the HARP software from end-diastole to end-systole. LVrot at basal and apical levels was used to calculate LVtor.

Statistical analysis. To assess the correlation of the measurements, we compared the LVtor and LVtor-v obtained by STI with those measured with tagged MRI and DTI by linear regression at isochronal time points, corresponding to the individual MRI frames. Analysis was conducted for the 400 ms after end-diastole (9.0 ± 1.2 frames) because reliable magnetic tagging persisted for this period. To compare isochronal LVtor and LVtor-v data while account-

JACC Vol. 45, No. 12, 2005
June 21, 2005:2034–41

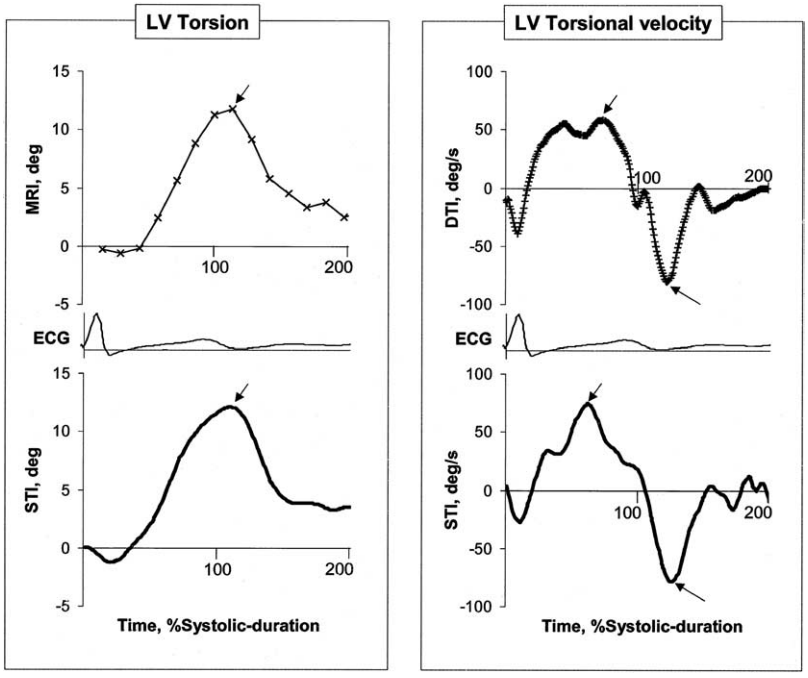

Figure 4. Left ventricular (LV) torsion and torsional profile curve by tagged magnetic resonance (MRI), Doppler tissue imaging (DTI), and speckle tracking imaging (STI) in a representative patient. **Arrows** indicate peak LV torsion and peak LV systolic and untwisting velocity.

ing for repeated observations per subject, we applied the following repeated-measures regression models (15).

$$R_{STI} = a + b * R_{MRI/DTI} + \sum c_i * D_i + \varepsilon, \quad (i = 1 \ldots n - 1)$$

where R_{STI} and $R_{MRI/DTI}$ are LVtor/LVtor-v by STI and MRI/DTI, respectively, D_i indicates dummy variables that code for individual subjects; a, b, and c are model parameters; and ε is the error term. The goodness-of-fit was assessed by within-subject correlation coefficient.

$$r = \sqrt{(SS_{cov} / (SS_{cov} + SS_{res}))}$$

where SS_{cov} and SS_{res} stand for sum of squares attributed to covariate or to residuals, respectively (16). To assess the correlation of peak LVtor and LVtor-v (peak systolic and untwisting velocity; Fig. 4) of the two modalities, simple linear regression analysis was performed. The accuracy of the LVtor and LVtor-v measurements with respect to the STI/MRI and STI/DTI data also were examined by a limits-of-agreement analysis (17). The bias was expressed as the mean difference between the two methods and the limits of agreement as two standard deviations of the difference of the two methods. To determine whether the difference in the values between the two methods was statistically significant, a paired *t* test was performed. Interobserver and intraobserver variability was examined in a blinded fashion in five randomly selected patients and expressed as correlation coefficients and coefficient of variation (CV) between measurements of two investigators and two readings (>1 month apart) as well as the mean and standard deviation of their differences. All of the statistical analysis was performed using Statistica 6.0 software (Statsoft, Tulsa, Oklahoma). All values were presented as mean ± SD. A $p < 0.05$ was taken to indicate statistical significance for all analyses.

RESULTS

The temporal resolution of MRI, STI, and DTI were 24 ± 3 Hz, 104 ± 12 Hz, and 136 ± 9 Hz, respectively. We could analyze LV torsional behavior by MRI and DTI method in all 15 patients, but the STI tracking score exceeded 2.5 in 2 patients; therefore, these patients were excluded from statistical analysis.

The profile curves of LVtor and LVtor-v by STI/MRI and STI/DTI in a representative case are shown in Figure 4. Regression analysis for measurement of LVtor and LVtor-v by STI (Fig. 5, upper panel) at isochronal time points, analyzed by repeated-measures regression models, indicates a strong correlation with those estimated by MRI and DTI ($r = 0.93$ and 0.76, respectively; $p < 0.0001$ for both modalities), with a standard error of the estimate of 2.26° and 22.6°/s (regression slope coefficient). The limits-of-agreement analysis (Fig. 5, lower panel) demonstrated no significant mean difference in measurement of LVtor and LVtor-v; the bias was 0.05 ± 2.42° for LVtor ($p = 0.82$) and 1.72 ± 24.6°/s for LVtor-v ($p = 0.27$). Comparing only the maximal torsion during systole, we also noted a strong correlation of LVtor between STI and MRI ($r = 0.86$, $p < 0.0001$) and LVtor-v between STI and DTI ($r = 0.94$, $p < 0.0001$).

Reproducibility of the STI method for LVtor. Interobserver measurements showed $r = 0.92$ for peak torsion (9.6 ± 2.4° vs. 9.1 ± 2.0°, CV = 10.5%) and $r = 0.81$ for peak

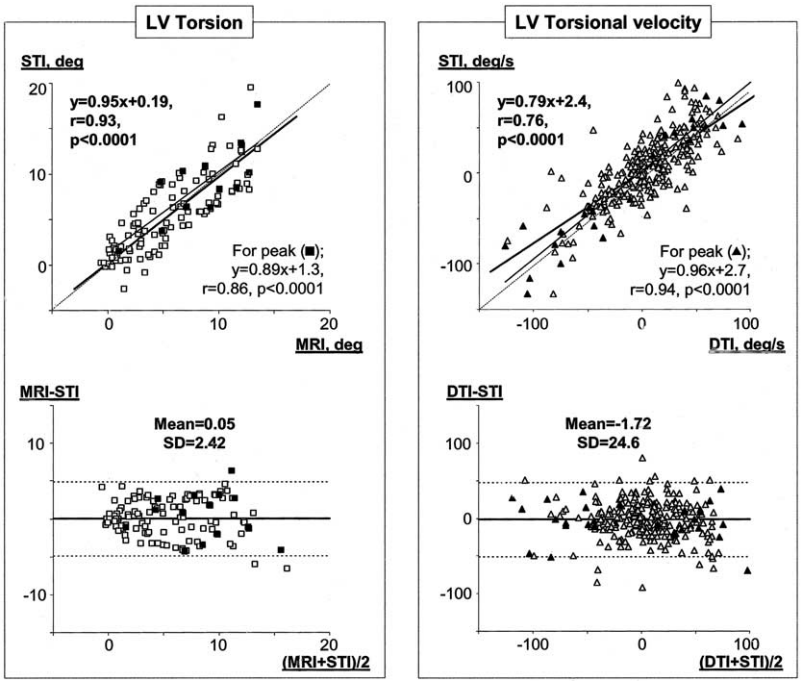

Figure 5. Correlation and agreement plots of torsion and torsional velocity between imaging modalities. The correlation using all the time points was analyzed by repeated-measures regression model, whereas the peak values **(filled symbols)** were analyzed by simple linear regression. DTI = Doppler tissue imaging; LV = left ventricular, MRI = magnetic resonance imaging; STI = speckle tracking imaging.

untwisting velocity (69 ± 10°/s vs. 66 ±9 °/s, CV = 9.0%). The error was random with no systematic trend observed ($p = 0.25$ and 0.38, respectively). Similarly, intraobserver variability showed $r = 0.92$ for peak torsion (9.1 ± 2.1° vs. 9.3 ± 1.8°, CV = 9.6%) and $r = 0.87$ for peak untwisting velocity (66 ± 9°/s vs. 68 ± 13°/s, CV = 8.1%), indicating satisfactory reproducibility for LVtor measurements by STI.

DISCUSSION

Imaging is one of the cornerstones of diagnosis in modern medical practice, and ultrasound is among the most mature technologies. In this study, we demonstrated that LV torsional deformation assessed by speckle tracking was quite consistent with those by MRI tissue tagging with acceptable bias and variability. Because the speckle-tracked data were obtained from relatively high-resolution two-dimensional images, the torsional velocity profile by the STI compared favorably with those by the DTI method, which was derived from primary detected velocity data with higher temporal resolution but with intrinsic directionality constraints common to all Doppler techniques.

Tagged MRI examinations have revealed important physiologic (18–21) and pathophysiologic findings for torsion as a relatively load-independent index of contractility and relaxation (22–25), making it an important reference standard to study cardiac biomechanics noninvasively. Improvements in this technique continue, such as the retagging at end-systole or using steady-state free precession with myocardial tagging (TrueFISP) (26), which can analyze LV deformation more robustly. Nevertheless, echocardiography is many-fold more available than MRI and therefore a more sophisticated assessment of LVtor by echo would be most welcome.

Ultrasound speckle tracking for assessment of LVtor.

ADVANTAGES. Many of the recent efforts to assess LVtor have used tissue velocity (Doppler) signals to assess rotational velocity at the base and apex (11). Researchers have demonstrated the ability of the DTI to characterize global and regional myocardial motion or deformation with high temporal resolution, but the angle dependency of Doppler is an unavoidable limitation (27–29) .

The alternative method for motion estimation proposed here is based on two-dimensional speckle tracking using time-domain processing, an approach that should be independent of both cardiac translation and angle-dependency. Mailloux et al. (30) proposed such an approach in 1987, but the absence of digitally stored high-frame-rate echo images led to unreliable results. Meunier and Bertrand (6) later reported a clear relationship between small tissue motion and the corresponding speckle pattern motion, demonstrating the potential for speckle tracking to study tissue dynamics. Success in the current implementation appears to derive from several factors, including the use of high-quality second harmonic images (31) that are acquired at high frame rates and are stored digitally in the original raw (scan line) format for analysis. The two-dimensional images were filtered nonlinearly before block-matching during processing (8–10), which helped to reduce the decorrelation score, i.e., the parameter used to indicate failure of

feature tracking (32). Torsional velocities derived from the relatively high frame rate data sets of STI were comparable with those derived from DTI. Untwisting velocity is thought to be a critical initial manifestation of active relaxation (18,21), making this measurement important for investigating diastole. The actual analytical process on the workstation is semiautomatic, with the time required to analyze LVtor for one patient typically <15 min, making this a tool not only for research use but also for clinical assessment.

DISADVANTAGES. There are, however, several shortcomings to the current STI approach. The STI analysis is inherently dependent on the two-dimensional echo image quality. Even among our 15 patients who were not "technically difficult," there were 2 patients whose decorrelation scores were too high for confident use. We also should note that the difference between STI and tagged MRI/DTI values was relatively large in some subjects, although the overall rotational profiles were quite similar.

Although speckle tracking has been reported previously (5–7), all of these methods have inferred tissue motion from isolated two-dimensional planes, whereas this motion is actually three-dimensional, which might remove some of the speckles from view by through-plane motion, particularly at the basal level. Fortunately the STI method only requires a statistically meaningful proportion of speckles to be present on successive frames, expecting some randomness superimposed on the true motion. Although we tried to define each slice by anatomical landmarks of the LV, we could not measure the exact distance between the scanned two levels. To overcome these problem, rudimentary three-dimensional echocardiographic speckle tracking already has been reported (33). Further developments in three-dimensional echocardiography may allow speckles to be tracked in all three dimensions, allowing an even more comprehensive assessment of ventricular function by echocardiography.

The B-mode image intrinsically has a lower signal-to-noise ratio than tissue Doppler (34), which may explain the slight underestimation of torsional velocity (slope = 0.79 in Fig. 5) in comparison with DTI-derived data; however, the peak torsional velocity showed excellent correlation (slope = 0.96).

Study limitations. Although we tried to collect patients who exhibited a variety of cardiac pathologies, the studied population was limited to patients who had a clinical indication for MRI examination. There was no way to guarantee absolute congruity of the short-axis levels used to assess LV torsion between echo and MRI, although the mitral valve and papillary muscles were used as landmarks in both modalities (11). The relatively low temporal resolution of MRI study in the current study might fail to detect the exact timing of end-systole, which might affect the analysis of the torsional profile. On average, however, end-systole occurred 33 ± 26 ms earlier by MRI than echo, which is within the single-frame durations of the MRI study (42 ms).

Clinical implications and conclusions. We have seen recent advances in understanding myocardial function at genetic/molecular levels (23,35,36). Integration of the new evidence in basic science and evolution in imaging technology must be matched with a new understanding of the importance of shape and fiber architecture to provide insights into disease that can lead to new therapy (1). Left ventricular torsion is important for normal ejection and suction and is an ingrained feature of the normal spread of excitation and connections between the fibers (3,37). Left ventricular torsion is a critical aspect of cardiac biomechanics (3,37–40), although it has been difficult to measure. The present study has validated the ability of STI to assess LV torsional deformation against MRI tissue tagging (which uses tissue displacement) and the DTI method (based on tissue velocity). Assessment of LVtor by the STI may help test hypotheses relating molecular changes and new macroscopic LV biomechanical concepts for better management of patients with heart failure.

Reprint requests and correspondence to: Dr. James D. Thomas, Department of Cardiovascular Medicine/F15, The Cleveland Clinic Foundation, 9500 Euclid Avenue, Cleveland, Ohio 44195. E-mail: thomasj@ccf.org.

REFERENCES

1. Buckberg GD, Weisfeldt ML, Ballester M, et al. Left ventricular form and function: scientific priorities and strategic planning for development of new views of disease. Circulation 2004;110:e333–6.
2. Mirro MJ, Rogers EW, Weyman AE, Feigenbaum H. Angular displacement of the papillary muscles during the cardiac cycle. Circulation 1979;60:327–33.
3. Arts T, Meerbaum S, Reneman RS, Corday E. Torsion of the left ventricle during the ejection phase in the intact dog. Cardiovasc Res 1984;18:183–93.
4. Wagner R, Smith S, Sandrik J, Lopez H. Statistics of speckle in ultrasound B-scans. IEEE Trans Sonics Ultrasonics 1983;30:156–63.
5. Bohs LN, Trahey GE. A novel method for angle independent ultrasonic imaging of blood flow and tissue motion. IEEE Trans Biomed Eng 1991;38:280–6.
6. Meunier J, Bertrand M. Ultrasonic texture motion analysis: theory and simulation. IEEE Trans Med Imaging 1995;14:293–300.
7. Bohs LN, Geiman B, Anderson M, Gebhart S, Trahey GE. Speckle tracking for multidimensional flow estimation. Ultrasonics 2000;38:369–75.
8. Behar V, Adam D, Lysyansky P, Friedman Z. The combined effect of nonlinear filtration and window size on the accuracy of tissue displacement estimation using detected echo signals. Ultrasonics 2004;41:743–53.
9. Reisner SA, Lysyansky P, Agmon Y, Mutlak D, Lessick J, Friedman Z. Global longitudinal strain: a novel index of left ventricular systolic function. J Am Soc Echocardiogr 2004;17:630–3.
10. Leitman M, Lysyansky P, Sidenko S, et al. Two-dimensional strain—a novel software for real-time quantitative echocardiographic assessment of myocardial function. J Am Soc Echocardiogr 2004;17:1021–9.
11. Notomi Y, Setser RM, Shiota T, et al. Assessment of left ventricular torsional deformation by Doppler tissue imaging: a validation study using tagged magnetic resonance imaging. Circulation 2005;111:1141–7.

12. Axel L, Dougherty L. MR imaging of motion with spatial modulation of magnetization. Radiology 1989;171:841–5.
13. Osman NF, Kerwin WS, McVeigh ER, Prince JL. Cardiac motion tracking using CINE harmonic phase (HARP) magnetic resonance imaging. Magn Reson Med 1999;42:1048–60.
14. Garot J, Bluemke DA, Osman NF, et al. Fast determination of regional myocardial strain fields from tagged cardiac images using harmonic phase MRI. Circulation 2000;101:981–8.
15. Glantz SA, Slinker BK. Analysis of variance and multiple regression. New York, NY: McGraw-Hill, Inc., 1990.
16. Bland JM, Altman DG. Calculating correlation coefficients with repeated observations: part 1—correlation within subjects. BMJ 1995;310:446.
17. Altman DG, Bland JM. Measurement in medicine: the analysis of method comparison studies. Statistician 1983;32:307–17.
18. Rademakers FE, Buchalter MB, Rogers WJ, et al. Dissociation between left ventricular untwisting and filling. Accentuation by catecholamines. Circulation 1992;85:1572–81.
19. Buchalter MB, Rademakers FE, Weiss JL, Rogers WJ, Weisfeldt ML, Shapiro EP. Rotational deformation of the canine left ventricle measured by magnetic resonance tagging: effects of catecholamines, ischaemia, and pacing. Cardiovasc Res 1994;28:629–35.
20. Moore CC, Lugo-Olivieri CH, McVeigh ER, Zerhouni EA. Three-dimensional systolic strain patterns in the normal human left ventricle: characterization with tagged MR imaging. Radiology 2000;214:453–66.
21. Dong SJ, Hees PS, Siu CO, Weiss JL, Shapiro EP. MRI assessment of LV relaxation by untwisting rate: a new isovolumic phase measure of tau. Am J Physiol Heart Circ Physiol 2001;281:H2002–9.
22. Stuber M, Scheidegger MB, Fischer SE, et al. Alterations in the local myocardial motion pattern in patients suffering from pressure overload due to aortic stenosis. Circulation 1999;100:361–8.
23. Bell SP, Nyland L, Tischler MD, McNabb M, Granzier H, LeWinter MM. Alterations in the determinants of diastolic suction during pacing tachycardia. Circ Res 2000;87:235–40.
24. Setser RM, Kasper JM, Lier ML, Starling RC, McCarthy PM, White RD. Persistent abnormal left ventricular systolic torsion in dilated cardiomyopathy after partial left ventriculectomy. J Thorac Cardiovasc Surg 2003;126:48–55.
25. Dong SJ, Hees PS, Huang WM, Buffer SA Jr., Weiss JL, Shapiro EP. Independent effects of preload, afterload, and contractility on left ventricular torsion. Am J Physiol 1999;277:H1053–60.
26. Zwanenburg JJ, Kuijer JP, Marcus JT, Heethaar RM. Steady-state free precession with myocardial tagging: CSPAMM in a single breathhold. Magn Reson Med 2003;49:722–30.
27. Urheim S, Edvardsen T, Torp H, Angelsen B, Smiseth OA. Myocardial strain by Doppler echocardiography. Validation of a new method to quantify regional myocardial function. Circulation 2000; 102:1158–64.
28. Castro PL, Greenberg NL, Drinko J, Garcia MJ, Thomas JD. Potential pitfalls of strain rate imaging: angle dependency. Biomed Sci Instrum 2000;36:197–202.
29. Gilman G, Khandheria BK, Hagen ME, Abraham TP, Seward JB, Belohlavek M. Strain rate and strain: a step-by-step approach to image and data acquisition. J Am Soc Echocardiogr 2004;17:1011–20.
30. Mailloux GE, Bleau A, Bertrand M, Petitclerc R. Computer analysis of heart motion from two-dimensional echocardiograms. IEEE Trans Biomed Eng 1987;34:356–64.
31. Caidahl K, Kazzam E, Lidberg J, et al. New concept in echocardiography: harmonic imaging of tissue without use of contrast agent. Lancet 1998;352:1264–70.
32. Kaluzynski K, Chen X, Emelianov SY, Skovoroda AR, O'Donnell M. Strain rate imaging using two-dimensional speckle tracking. IEEE Trans Ultrason Ferroelectr Freq Control 2001;48:1111–23.
33. Meunier J. Tissue motion assessment from 3D echographic speckle tracking. Phys Med Biol 1998;43:1241–54.
34. Wells P. Ultrasonic imaging of the human body. Rep Prog Phys 1999;62:671–722.
35. Davis JS, Hassanzadeh S, Winitsky S, et al. The overall pattern of cardiac contraction depends on a spatial gradient of myosin regulatory light chain phosphorylation. Cell 2001;107:631–41.
36. Davis JS, Hassanzadeh S, Winitsky S, Wen H, Aletras A, Epstein ND. A gradient of myosin regulatory light-chain phosphorylation across the ventricular wall supports cardiac torsion. Cold Spring Harb Symp Quant Biol 2002;345–52.
37. Torrent-Guasp F, Kocica MJ, Corno A, et al. Systolic ventricular filling. Eur J Cardiothorac Surg 2004;25:376–86.
38. Harvey W. An anatomical disposition on the motion of the heart and blood in animals, 1628. In: Willis FA, Keys TE, editors. Cardiac Classics. London, England: Henry Kimpton, 1941:19–79.
39. Streeter DD, Jr., Spotnitz HM, Patel DP, Ross J, Jr., Sonnenblick EH. Fiber orientation in the canine left ventricle during diastole and systole. Circ Res 1969;24:339–47.
40. Ingels NB, Jr., Daughters GT, 2nd, Stinson EB, Alderman EL. Measurement of midwall myocardial dynamics in intact man by radiography of surgically implanted markers. Circulation 1975; 52:859–67.